

## Article

# Fluorine-Free Single-Component Polyelectrolyte of Poly(ethylene glycol) Bearing Lithium Methanesulfonylsulfonimide Terminal Groups: Effect of Structural Variance on Ionic Conductivity

Bungo Ochiai <sup>\*</sup>, Koki Hirabayashi, Yudai Fujii and Yoshimasa Matsumura <sup>†</sup>

Graduate School of Science and Engineering, Yamagata University, Yonezawa 990-8510, Japan; ydi.fujii@gmail.com (Y.F.); yoshimasa.matsumura@oit.ac.jp (Y.M.)

<sup>\*</sup> Correspondence: ochiai@yz.yamagata-u.ac.jp; Tel.: +81-238-26-3092

<sup>†</sup> Current Address: Department of Applied Chemistry, Faculty of Engineering, Osaka Institute of Technology, Osaka 535-8585, Japan.

**Abstract:** Fluorine-free single-component polyelectrolytes were developed via the hybridization of lithium methanesulfonylsulfonimide (LiMSSI) moieties to poly(ethylene glycol) (PEG) derivatives with different morphologies, and the relationship between the structure and its ionic conductivity was investigated. The PEG-LiMSSI derivatives with one, two, and three LiMSSI end groups were prepared via the concomitant Michael-type addition and lithiation of PEGs and *N*-methanesulfonylvinyllsulfonimide. The ionic conductivity at 60 °C ranged from  $1.8 \times 10^{-7}$  to  $2.0 \times 10^{-4}$  S/cm. PEG-LiMSSI derivatives with one LiMSSI terminus and with two LiMSSI termini at both ends show higher ionic conductivity, that is as good as fluorine-free single-component polyelectrolytes, than that with two LiMSSI termini at one end and that with three LiMSSI termini.

**Keywords:** lithium ion; poly(ethylene glycol); battery; ion conductivity; polyelectrolyte; sulfonyl imide



**Citation:** Ochiai, B.; Hirabayashi, K.; Fujii, Y.; Matsumura, Y. Fluorine-Free Single-Component Polyelectrolyte of Poly(ethylene glycol) Bearing Lithium Methanesulfonylsulfonimide Terminal Groups: Effect of Structural Variance on Ionic Conductivity. *Technologies* **2024**, *12*, 65. <https://doi.org/10.3390/technologies12050065>

Academic Editor: Piero Cosseddu

Received: 9 April 2024

Revised: 30 April 2024

Accepted: 7 May 2024

Published: 9 May 2024



**Copyright:** © 2024 by the authors. Licensee MDPI, Basel, Switzerland. This article is an open access article distributed under the terms and conditions of the Creative Commons Attribution (CC BY) license (<https://creativecommons.org/licenses/by/4.0/>).

## 1. Introduction

Lithium-ion batteries are used in a wide range of applications, from large batteries for automobiles and smart grids to small batteries for mobile devices. In recent years, polymer-type batteries, which have a lower risk of leakage and thus allow for simpler packaging, have become more widespread [1–4]. Their disadvantage is their low ionic conductivity. In addition, typical gel electrolytes, consisting of polymers and low-molecular-weight lithium salts, suffer from the predominant transference of anions over lithium cations because lithium cations are ligated by polymers such as poly(ethylene glycol) (PEG) to reduce their relative mobility. To overcome this problem, polymers with immobilized anion structures in their backbones have been designed to suppress the migration of anions. Carboxylates, sulfonates, sulfonamides, and trifluoromethanesulfonylsulfonimides are typical anionic structures for linking to organic backbones, and various single-component polyelectrolytes without low-molecular-weight anions have been developed.

Anions hybridized with PEG for conducting lithium cations are typical examples. Ohno et al. developed a series of single-component electrolytes of PEG derivatives with carboxylate [5], sulfonate [6,7], and sulfonamide [8,9] termini with ionic conductivities of  $10^{-6}$ – $10^{-7}$  S/cm at ambient temperatures. The migration of anions is successfully suppressed by reducing the mobility of anions, but the total ionic conductivities are insufficient. Various researchers have developed PEG derivatives with other anions to improve ionic conductivity. Aluminates consisting of PEG chains and fluorinated anions developed by Fujinami et al. show ionic conductivities of  $10^{-5}$  S/cm at room temperature [10]. Subsequently, borate analogs were developed and showed similar ionic conductivities [11–14].

Despite the improved ionic conductivity, the low stabilities of aluminum and boron alkoxides are problematic. The introduction of one alkyl chain, one fluorinated alkoxy group, and two tri(ethylene glycol) chains on boron resulted in higher stability and ion conductivity ( $>10^{-4}$  S/cm $^{-1}$  at room temperature) [15]. PEGs with bis(fluoroalkanesulfonyl)imide ends [16,17] and a 1,2,3-triazolate [18] end were also designed and exhibited ionic conductivities of  $10^{-6}$  and  $10^{-7}$  S/cm at room temperature, respectively. Block copolymers composed of PEG chains and styrene-based fluorinated polyanions [19–21] and cross-linked PEG derivatives with lithium sulfonate and trifluoromethanesulfonylsulfonimide ends [22] have also been developed.

Most polymers with higher ionic conductivity contain fluorinated structures to stabilize anions, as described later. However, the fluorinated organic groups increase the environmental risk [23,24] and the price. Accordingly, both low-molecular-weight and polymeric fluorine-free electrolytes are in high demand [25–31]. For the stable hybridization of fluorine-free organic structures and anions, we focused on bis(alkanesulfonyl)imide moieties that carry the anion on the nitrogen atom delocalized by two sulfonimide groups with strong electron-withdrawing properties. Lithium bis(alkanesulfonyl)imide derivatives have good ionic conductivities despite their low solubilities [25].

We applied the lithium methanesulfonylsulfonimide (LiMSSI) moieties to polymers with copolymers of PEG methacrylate (PEGMA) and lithium-*N*-methanesulfonylvinylylsulfonimide (LiMSVSI), a vinyl monomer with a similar structure to lithium trifluoromethanesulfonyl sulfonimide (LiTFSI), which exhibit good ionic conductivities of  $8.4 \times 10^{-5}$  and  $9.2 \times 10^{-4}$  S/cm at 25 and 90 °C, respectively [31]. The problem of the poor solubility was overcome by copolymerization. However, LiMSVSI has a low radical polymerizability, which limits the density of the lithium salt structure lower.

During the synthesis of LiMSVSI, we found that ethanol nucleophilically adds to the vinyl group of *N*-methanesulfonylvinylylsulfonimide (MSVSI) via the Michael-type addition with the simultaneous lithiation of the sulfonimide group. We extended this finding to the design of PEGs bearing LiMSSI terminal groups without additional salts and solvents. Furthermore, different derivatives were synthesized and evaluated to investigate the effects of factors on the ionic conductivities. The LiMSSI-terminated PEG derivatives examined are PEGs with one, two, and three terminal LiMSSI groups with different molecular weights (Figure 1). In this study, we clarified the effect of the structural variance, namely, how the molecular weight of the PEG segment, the modification ratio of terminal LiMSSI, the number of terminal LiMSSI groups, and the morphological arrangement of terminal LiMSSI groups affect the ionic conduction behavior and the glass transition temperature ( $T_g$ ), a controlling factor for ionic conductivity, of PEGs with terminal LiMSSI structures.

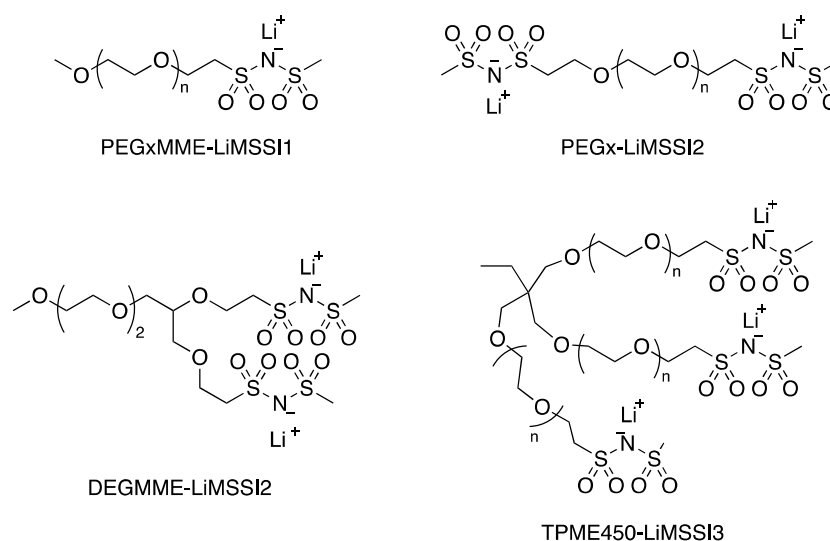


**Figure 1.** The PEGs with LiMSSI termini examined in this study.

## 2. Materials and Methods

### 2.1. Materials

All the reagents were used as received. MSVSI [30] and 3-[2-(2-methoxyethoxy)ethoxy]-1,2-propanediol (DMEMME diol) [32] were prepared as reported. LiOH monohydrate, tetrahydrofuran (THF), methanol, acetone, ethyl acetate, methylene dichloride, PEG with an  $M_n$  of 1000 (PEG1000), and diethyl carbonate (DEC) were purchased from Kanto Chemical (Tokyo, Japan). PEG monomethyl ether with a number-average molecular weight ( $M_n$ ) of 400 (PEG400MME), PEG monomethyl ether with an  $M_n$  of 1000 (PEG1000MME), PEG with an  $M_n$  of 200 (PEG200), PEG with an  $M_n$  of 400 (PEG400), and LiTFSI were purchased from Tokyo Chemical Industry (Tokyo, Japan). Trimethylolpropane ethoxylate ( $M_n = ca. 450$ ) (TMPE450) was purchased from Sigma-Aldrich (St. Louise, MO, USA). Ethylene carbonate (EC) was purchased from Wako Pure Chemical (Osaka, Japan).

### 2.2. Measurements

#### 2.2.1. Instruments

$^1\text{H}$  NMR spectra were measured on a JEOL (Tokyo, Japan) ECX-400 spectrometer using  $\text{D}_2\text{O}$  as the solvent (23–25 °C, relaxation delay = 5 s, 8 scans). The residual solvent signal of DHO was used as the internal reference.  $^7\text{Li}$  NMR spectra were measured on a JEOL (Tokyo, Japan) ECX-500 spectrometer using  $\text{D}_2\text{O}$  as the solvent (23–25 °C, relaxation delay = 2 s, 24 scans). Differential scanning calorimetry (DSC) measurements were performed on a Seiko (Tokyo, Japan) DSC-220 instrument under a nitrogen atmosphere (10 °C/min,  $\text{N}_2$ , with a second heating scan after heating to 100 °C and cooling to –80 °C at 10 °C/min). Cyclic voltammetric (CV) analyses were carried out on a CH Instruments (Austin, TX, USA) CHI704E potentiostat at the scan rate of 0.1 V/s. All the measurements were performed in a 1.0 M LiTFSI solution of EC/DEC ( $v/v = 3/7$ ) at ambient temperature using a three-electrode system, with each solution being purged with nitrogen prior to measurement. The working electrode was a Pt disk ( $\phi = 5$  mm, BAS, Tokyo, Japan), the counter electrode was a Pt wire ( $\phi = 0.5$  mm, BAS, Tokyo, Japan), and the reference electrode was an Ag wire ( $\phi = 1$  mm, Nilaco, Tokyo, Japan).

#### 2.2.2. Measurement of Ion Conductivity

Ionic conductivities were measured using a Hioki (Nagano, Japan) 3532-80 electrochemical impedance spectrometer. A two-point-probe conductivity cell with two platinum plate electrodes was fabricated. The cell was placed in a nitrogen-filled plastic bag in an EYELA (Tokyo, Japan) VOS-300VD thermo-controlled chamber. The samples were dried at 90 °C under a vacuum for at least 10 h prior to the measurement and were treated under a nitrogen atmosphere. The chamber temperature was raised to approximately 100 °C, and the temperature around the samples was measured using a digital thermometer placed aside from the samples. The samples were annealed for 1 h, and the chamber temperature was lowered. Ionic conductivity was monitored as a gradual decrease in the temperature of the samples. Ionic conductivity ( $\sigma$ ) was calculated from following Equation (1).

$$\sigma = d/(LWR) \quad (1)$$

In the equation,  $d$ ,  $L$ ,  $W$ , and  $R$  are the distance between the two electrodes (cm), the length of electrode (cm), the width of electrode (cm), and the resistance value ( $\Omega$ ), respectively.

### 2.3. Synthesis of Polymers

#### 2.3.1. Synthesis of DEGMME-LiMSSI2

DEGMME diol (58.8 mg, 300  $\mu\text{mol}$ ), MSVSI (111 mg, 600  $\mu\text{mol}$ ), and lithium hydroxide monohydrate (50.4 mg, 600  $\mu\text{mol}$ ) were added to a 20 mL round-bottom flask. Then, the flask was degassed and purged with nitrogen. The mixture was magnetically stirred in an oil bath maintained at 100 °C for 48 h. The resulting viscous material was dissolved in THF, and the soluble portion was collected via filtration. The solvent was removed using an

evaporator, and MSVSI (93–185 mg, 0.50–1.00 mmol) was added again and stirred at 100 °C for 48 h. This procedure was repeated two or three times until the introduction efficiency of the LiMSSI group became constant.

For purification, THF was first added. The soluble portion was collected to remove LiOH, and THF was evaporated off under a vacuum. Next, the product was re-precipitated using 15 mL of THF as a good solvent and 300 mL of ethyl acetate as a poor solvent. The resulting dispersion was centrifuged, and the supernatant was removed. The precipitate was collected via dissolving in methanol to give a DEGMME derivative with two LiMSSI termini (DEGMME-LiMSSI2) (yield = 20 mg and 12%, introduction ratio of LiMSSI termini 89%).

<sup>1</sup>H-NMR (400 MHz, D<sub>2</sub>O, δ in ppm): 3.38 (s, 3H, -SO<sub>2</sub>CH<sub>3</sub>), 3.43 (t, *J* = 6.2 Hz, 2H, >CHOCH<sub>2</sub>CH<sub>2</sub>SO<sub>2</sub>-), 3.50 (t, *J* = 6.2 Hz, 2H, -CH<sub>2</sub>OCH<sub>2</sub>CH<sub>2</sub>SO<sub>2</sub>-), 3.50–3.80 (br, polyether backbone), 3.96 (t, *J* = 5.5 Hz, 2H, -CH<sub>2</sub>OCH<sub>2</sub>CH<sub>2</sub>SO<sub>2</sub>-), 4.00 (t, *J* = 5.5 Hz, 2H, >CH<sub>2</sub>OCH<sub>2</sub>CH<sub>2</sub>SO<sub>2</sub>-).

<sup>7</sup>Li-NMR (194 MHz, D<sub>2</sub>O, δ in ppm): 2.96 (N-Li).

### 2.3.2. Synthesis of TMPE450-LiMSSI3

TPME450 (900 mg, 2.00 mmol), MSVSI (1.11 g, 6.00 mmol), and lithium hydroxide monohydrate (378 mg, 9.00 mmol) were added to a 20 mL round-bottom flask. Then, the flask was degassed and purged with nitrogen. The mixture was magnetically stirred in an oil bath maintained at 100 °C for 48 h. The resulting viscous material was dissolved in THF, and the soluble portion was collected via filtration. The solvent was removed using an evaporator, and MSVSI (93–185 mg, 0.50–1.00 mmol) was added again and stirred at 100 °C for 48 h. This procedure was repeated two or three times until the quantitative introduction of the LiMSSI group.

For purification, acetone was first added, and the mixture was sonicated for 1 h. The soluble portion was collected to remove LiOH, and acetone was evaporated off under a vacuum. Next, the product was re-precipitated using 15 mL of acetone as a good solvent and 300 mL of methylene dichloride as a poor solvent. The resulting dispersion was centrifuged, and the supernatant was removed. The precipitate was collected via dissolving in methanol to give a TPME450 derivative with three LiMSSI termini (TPME450-LiMSSI3) (yield = 530 mg and 25%, introduction ratio of LiMSSI termini > 86%).

<sup>1</sup>H-NMR (400 MHz, D<sub>2</sub>O, δ in ppm): 0.85 (t, *J* = 7.5 Hz, 3H, -CH<sub>2</sub>CH<sub>3</sub>), 1.35 (q, *J* = 7.5 Hz, 2H, -CH<sub>2</sub>CH<sub>3</sub>), 3.08 (s, 3H, -SO<sub>2</sub>CH<sub>3</sub>), 3.42 (s, EtC(CH<sub>2</sub>O)<sub>3</sub>-), 3.49 (t, *J* = 6.4 Hz, 2H, -CH<sub>2</sub>CH<sub>2</sub>SO<sub>2</sub>-), 3.63–3.75 (4nH, -OCH<sub>2</sub>CH<sub>2</sub>O-), 3.93 (t, *J* = 6.3 Hz, 2H, -CH<sub>2</sub>CH<sub>2</sub>SO<sub>2</sub>-).

<sup>7</sup>Li-NMR (194 MHz, D<sub>2</sub>O, δ in ppm): 2.96 (N-Li).

### 2.3.3. Synthesis of PEG200-LiMSSI2 (Typical Procedure)

PEG with an *M<sub>n</sub>* of 200 (PEG200) (2.00 g, 10.0 mmol), MSVSI (3.70 g, 20.0 mmol), and lithium hydroxide monohydrate (1.68 g, 40.0 mmol) were added to a 20 mL round-bottom flask. Then, the flask was degassed and purged with nitrogen. The mixture was magnetically stirred in an oil bath maintained at 100 °C for 48 h. The resulting viscous material was dissolved in methylene dichloride, and the soluble portion was collected via filtration. The solvent was removed using an evaporator, and MSVSI (93–185 mg, 0.50–1.00 mmol) was added again and stirred at 100 °C for 48 h. This procedure was repeated two or three times.

For purification, methylene chloride was first added to the product and sonicated for 1 h. The soluble portion was collected, and methylene dichloride was removed under a vacuum. Next, the product was re-precipitated using 15 mL of ethanol as a good solvent and 300 mL of ethyl acetate as a poor solvent. The resulting dispersion was centrifuged, and the supernatant was removed. The precipitate was collected via dissolving in methanol to give a PEG200 derivative with two LiMSSI termini (PEG200-LiMSSI2) (yield = 0.84 g and 34%, introduction ratio of LiMSSI termini > 99%).

<sup>1</sup>H-NMR (400 MHz, D<sub>2</sub>O, δ in ppm): 3.01 (s, 3H, -SO<sub>2</sub>CH<sub>3</sub>), 3.53 (t, *J* = 6.4 Hz, 2H, -CH<sub>2</sub>CH<sub>2</sub>SO<sub>2</sub>-), 3.59–3.69 (-4nH, -OCH<sub>2</sub>CH<sub>2</sub>O-), 3.88 (t, *J* = 6.4 Hz, 2H, -CH<sub>2</sub>SO<sub>2</sub>-).  
<sup>7</sup>Li-NMR (194 MHz, D<sub>2</sub>O, δ in ppm): 2.96 (N-Li).

### 2.3.4. Synthesis of Other Polymers Bearing LiMSSI Termini

All the polymers were synthesized following the method described for PEG200-LiMSSI2 (2.00 g, 10.0 mmol). The results are summarized in Table 1, and the <sup>1</sup>H NMR spectra are indicated in the Supplementary Materials (Figures S1–S6).

**Table 1.** The LiMSSI-terminated PEG examined in this research.

Polymer	PEG	Introduction Efficiency (%) <sup>a</sup>	[Li]/[O] <sup>b</sup>	Yield (%)	<i>T<sub>g</sub></i> (°C) <sup>c</sup>	<i>T<sub>m</sub></i> (°C) <sup>c</sup>
PEG400MME-LiMSSI1	PEG400MME	>99	0.10	45 <sup>d</sup>	−48	n.o. <sup>h</sup>
PEG1000MME-LiMSSI1	PEG1000MME	95	0.045	50 <sup>d</sup>	−56	27
PEG200-LiMSSI2	PEG200	95	0.46	ca. 40 <sup>d,e</sup>	−18	n.o. <sup>h</sup>
		>99	0.48	34 <sup>d</sup>	9	n.o. <sup>h</sup>
PEG400-LiMSSI2	PEG400	91	0.19	70 <sup>d</sup>	−30	n.o. <sup>h</sup>
		>99	0.21	ca. 15 <sup>d,e</sup>	−11	n.o. <sup>h</sup>
PEG1000-LiMSSI2	PEG1000	>99	0.082	70 <sup>d</sup>	−18	n.o. <sup>h</sup>
DEGMME-LiMSSI2	DEGMME-diol	89	0.36	12 <sup>f</sup>	−52	n.o. <sup>h</sup>
TMPE450-LiMSSI3	TPME450	86	0.30	25 <sup>g</sup>	−18	n.o. <sup>h</sup>

<sup>a</sup> Determined via <sup>1</sup>H NMR spectroscopy (400 MHz, D<sub>2</sub>O). <sup>b</sup> Molar ratio of Li to O in ethylene glycol units (the O in the sulfonamide structures was omitted from the calculation). <sup>c</sup> Determined by DSC (10 °C/min, second heating scan, N<sub>2</sub>). <sup>d</sup> The isolated yield after reprecipitation with ethyl acetate from an ethanol solution. <sup>e</sup> The approximate value due to loss during the repeated confirmation of introduction efficiency. <sup>f</sup> The isolated yield after reprecipitation with ethyl acetate from a THF solution. <sup>g</sup> The isolated yield after reprecipitation with CH<sub>2</sub>Cl<sub>2</sub> from an acetone solution. <sup>h</sup> Not observed.

## 3. Results and Discussion

### 3.1. Synthesis of PEGs with LiMSSI Termini

Through the concomitant Michael addition of the terminal hydroxy groups of PEG and lithiation, we synthesized PEGs with one LiMSSI terminus (PEGxMME-LiMSSI1) and two LiMSSI termini at both ends (PEGx-LiMSSI2) using PEG monomethyl ether and PEG with both terminal hydroxy groups, respectively, where x denotes the number-average molecular weight of PEG. Furthermore, a three-terminated oligo(ethylene glycol) TMPE450-LiMSSI3 and a diethylene glycol derivative bearing two LiMSSI termini at one end (DEGMME-LiMSSI2) were synthesized via the reaction of trimethylolpropane ethoxylate (average *M<sub>n</sub>* = 450) (TMPE450) and DEGMME diol, respectively. An excess amount (1.0–1.5 equivalents) of MSVSI and an excess amount (2–3 equivalents) of lithium hydroxide monohydrate were added to the terminal hydroxyl group of each PEG, and the reaction was carried out at 100 °C for 48 h under a nitrogen atmosphere. If the introduction efficiencies were insufficient, the reaction was further carried out by adding an excess amount of MSVSI and lithium hydroxide monohydrate. Purification methods were adjusted based on the solubility of each polymer.

As an example, Figure 2a shows the <sup>1</sup>H-NMR spectrum of PEG200-LiMSSI2, indicating a peak at 3.01 ppm derived from the methyl group of the methanesulfonyl group (a) and peaks at 3.42 (b) and 3.88 ppm (c) derived from the ethylene group adjacent to the sulfonyl group along with the peak of the PEG unit. The peak (f) derived from the methylene group adjacent to the hydroxyl group at 3.57 ppm is almost unobservable, indicating that the hydroxy group is almost completely consumed. The fact that the incorporation ratio was higher than 99% was confirmed by the integral ratio of the peak derived from the LiMSSI group to the peak derived from the PEG chain at 3.6 ppm. In addition, a peak at

2.96 ppm was observed in the  $^7\text{Li}$ -NMR spectrum, indicating the presence of lithium salt moieties (Figure 2b).

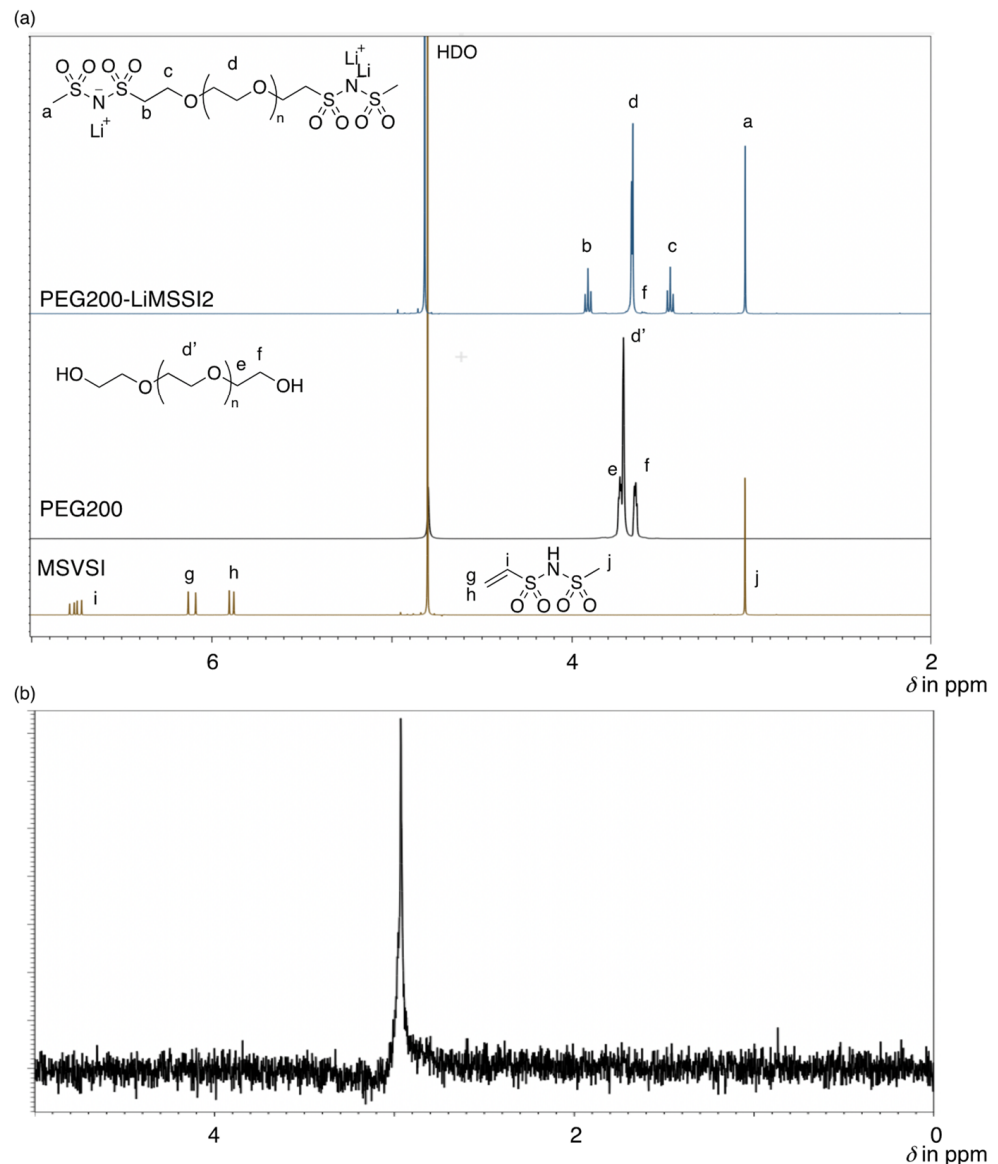


**Figure 2.** (a) The  $^1\text{H}$  NMR spectra of MSVSI, PEG200, and PEG200-LiMSSI2 (400 MHz); and the (b)  $^7\text{Li}$  NMR spectrum of PEG200-LiMSSI2 (194 MHz) ( $\text{D}_2\text{O}$ ).

### 3.2. Properties of PEGs with LiMSSI Termini

#### 3.2.1. Electrochemical Stability

The electrochemical stability of PEG200-LiMSSI2 was evaluated by CV measurements using EC/DEC ( $v/v = 3/7$ ) containing 1.0 M of LiTFSI as the electrolyte solution, silver nitrate electrolyte as the reference electrode, a platinum disk as the working electrode, and a platinum wire as the counter electrode at a sweep rate of 0.1 V/s. The cyclic voltammogram of the electrolyte solutions of PEG200-LiMSSI2 (Figure 3) showed only peaks around 2.5 V and  $-3.5$  V, originating from the oxidation and reduction of the electrolyte. None of the oxidation and reduction peaks of the polymers were observed, indicating that PEG200-LiMSSI2 is electrochemically stable enough in the electrochemical window of the electrolyte. The cyclic voltammograms of DEGMME-LiMSSI2 and TMPE450-LiMSSI3, which have different structures, were identical to that of PEG200-LiMSSI2, indicating their electrochemical stability (Figure S7).

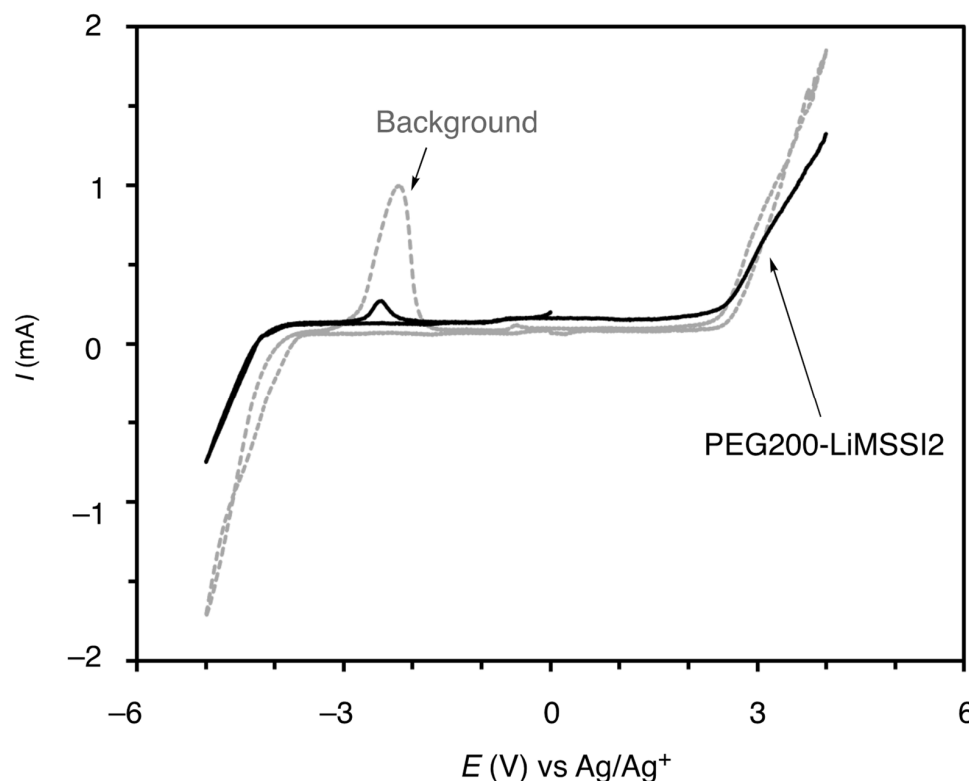


**Figure 3.** Cyclic voltammograms of PEG200-LiMSSI2 (plain) and background (dashed) in a 1.0 M EC/DEC ( $v/v = 3/7$ ) solution of LiTFSI; reference electrode, Ag/Ag<sup>+</sup>; working electrode, Pt disk ( $\varphi = 1.6$  mm); counter electrode, Pt wire ( $\varphi = 0.5$  mm); sweep rate = 0.1 V/s.

### 3.2.2. Thermal Behaviors

The glass transition, crystallization, and melting behavior of the synthesized PEG-LiMSSI were analyzed using DSC. The analysis was performed in the second heating scan at a heating rate of 10 °C/min after the first heating scan to 100 °C, followed by the cooling scan to −80 °C at a cooling rate of 10 °C/min (Figure S8). The  $T_g$  and melting temperature ( $T_m$ ) are summarized in Table 1.

The crystallization of the PEG chains was suppressed by the terminal LiMSSI structure as previously reported in PEG derivatives with anionic termini [6–9]. In the thermograms of PEG $_x$ -LiMSSI2 ( $x = 200, 400,$  and  $1000$ ) and PEG $_x$ MME-LiMSSI1 ( $x = 200$  and  $400$ ), no endothermic peaks derived from the melting of PEG chain crystals were observed, indicating that the terminal LiMSSI structure completely suppressed the crystallization of PEG. DEGMMME-LiMSSI2 and TMPE450-LiMSSI3, whose oligoethers are not crystalline, were also amorphous within the investigated temperature range. On the other hand, in the DSC curve of PEG1000MME-LiMSSI, an exothermic peak resulting from cold crystallization was observed at around −35 °C, and an endothermic peak resulting from the melting of PEG chains was observed at 27 °C. These data indicate that sufficient lengths of PEG chains, apart from the LiMSSI terminus, are necessary for crystallization.

The terminal LiMSSI structure increased the  $T_g$  through intermolecular ionic interactions. For the same molecular weight of PEG, the  $T_g$  was higher for the doubly terminated PEG. For example, the  $T_g$  of the mono-terminated PEG400MME-LiMSSI1 and the doubly terminated PEG400-LiMSSI2 with the quantitative introduction efficiency were −48 °C and −11 °C, respectively. The introduction efficiency also affects the  $T_g$ . We prepared PEG200-LiMSSI2 and PEG400-LiMSSI2 with different introduction efficiencies and found that the  $T_g$ s are increased by the quantitative introduction of the LiMSSI ends. The  $T_g$  of TPME450-LiMSSI3 is also higher than that of PEG400MME-LiMSSI1 and is identical to that of PEG400-LiMSSI2 with a closer introduction efficiency. Considering the lower introduction efficiency and higher molecular weight of TPME450-LiMSSI3, we suggest that

the three ionic end groups in one molecule resulted in ionic cross-linkage, which restricts the movement of ions and ether chains.

### 3.2.3. Ionic Conductivity

The effects of PEG's molecular weight, and the introduction efficiency, number, and morphological arrangement of the LiMSSI structure on the ionic conductivity were comprehensively evaluated by comparing the ionic conductivity. The ionic conductivity was measured at each temperature during cooling from 100 °C under nitrogen. Prior to measurement, the samples were annealed at 90 °C under reduced pressure for half a day and then brought to a steady state under nitrogen.

The effect of PEG's molecular weight on ionic conductivity was evaluated by changing the PEG molecular weight ( $x$ ) of PEG $x$ -LiMSSI2 with LiMSSI structures at both ends to 200, 400, and 1000 (Figure 4).

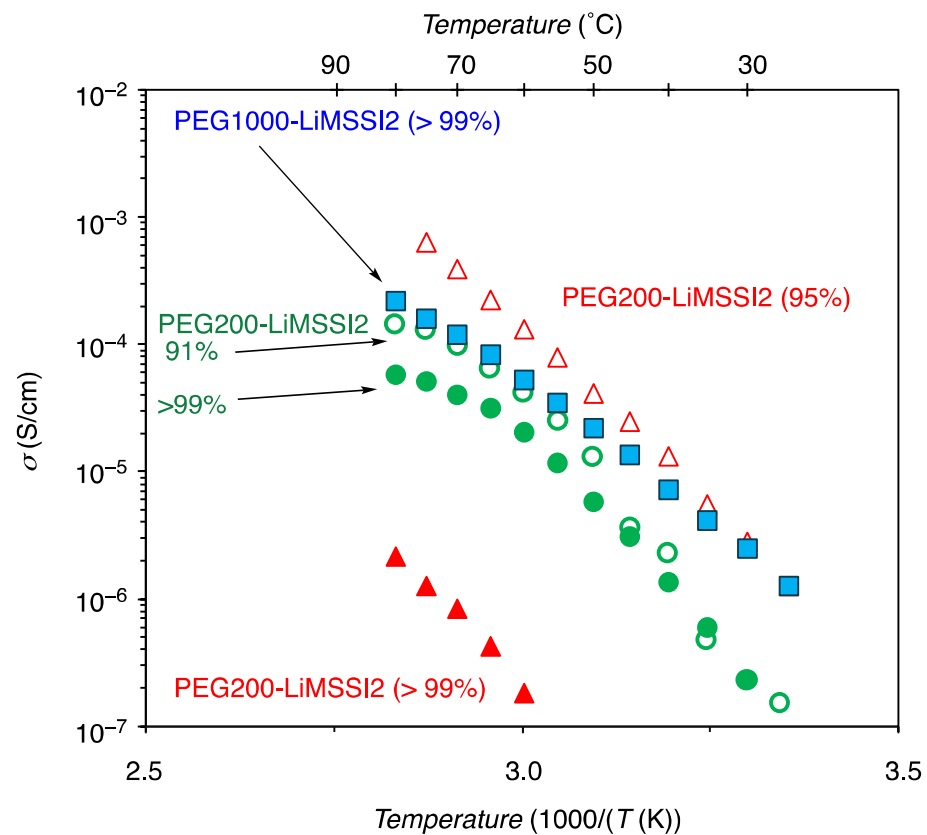


**Figure 4.** The ionic conductivity of PEG200-LiMSSI2 (red triangle) with an LiMSSI introduction efficiency of 95% (opened) and >99% (filled), PEG400-LiMSSI2 (green circle) with an LiMSSI introduction efficiency of 91% (opened) and >99% (filled), and PEG1000-LiMSSI2 with an LiMSSI introduction efficiency of >99% (blue square).

The ionic conductivity of PEG $x$ -LiMSSI2 ( $x = 200, 400, \text{ and } 1000$ ) with an introduction efficiency higher than 95% (filled marks in Figure 4) increased with an increasing PEG molecular weight. This trend is consistent with previously developed PEGs with ionic ends [6–9] and correlates with  $T_g$ . The LiMSSI structure is sterically stiffer than the PEG chain and forms ionic interactions. These structural and chemical factors both restrict the mobility of the polymer chains and thus reduce the mobility of the lithium ions.

The ionic conductivities of PEG200-LiMSSI2 and PEG400-LiMSSI2 with lower introduction efficiencies were also investigated (open marks in Figure 4). In both cases, the ionic conductivities were higher than those of the analogs with the higher introduction efficiencies. This effect of the introduction efficiency was striking. The approximately

5% decrease in the introduction efficiency decreased the ionic conductivity by three orders of magnitude, even though the [Li]/[O] ratios were almost identical. The  $T_g$ s also became significantly higher with the slight decrease in the introduction efficiency. This difference will be discussed later.

We compared the ionic conductivities of PEG400MME-LiMSSI, PEG400-LiMSSI2, and TMPE450-LiMSSI3 with one, two, and three terminal LiMSSI structures, respectively, with molecular weights of the PEG chains being approximately 400 to study the effect of different end groups (Figure 5).

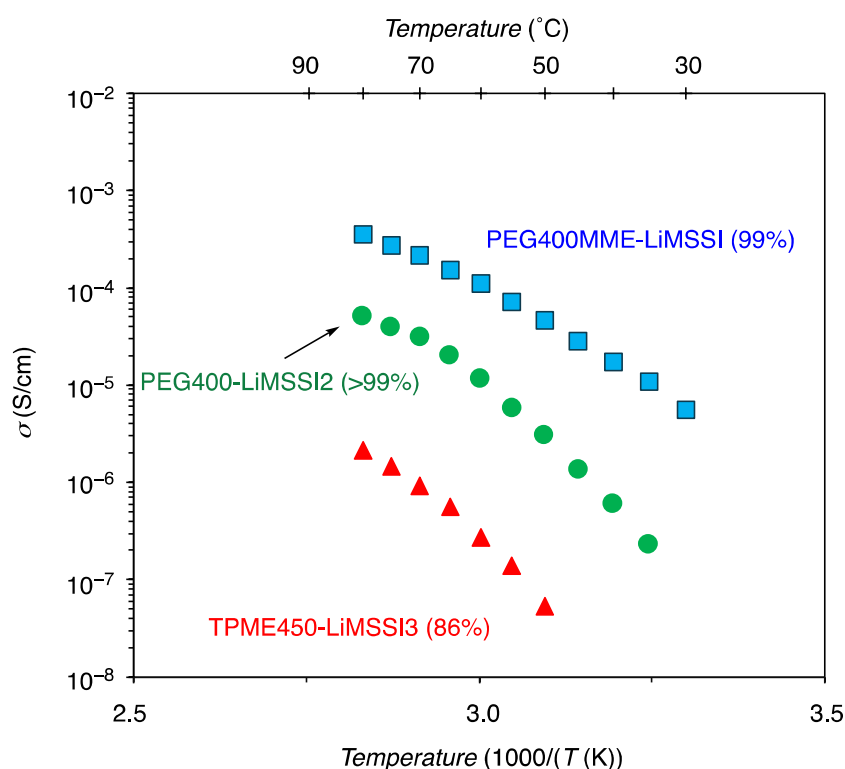


**Figure 5.** The ionic conductivities of PEG400-MME-LiMSSI (blue square), PEG400-LiMSSI2 (green circle), and TPME450-LiMSSI3 (red triangle).

The ionic conductivity decreased as the number of terminal LiMSSI groups increased. In particular, the trifunctional TMPE450-LiMSSI3 is more than two orders of magnitude lower than the monofunctional PEG400MME-LiMSSI and the difunctional PEG400-LiMSSI2. The  $T_g$  also increased as the number of terminal LiMSSI groups increased. As with the PEG molecular weights, the decrease in ionic conductivity and the increase in  $T_g$  were attributed to an increase in the [Li]/[O] ratio and the density of the terminal LiMSSI groups, resulting in more interchain interactions. Therefore, we compared the ionic conductivity of PEG200-LiMSSI2, which has a higher [Li]/[O] ratio than that of TMPE450-LiMSSI3. As a result, their ionic conductivities were almost equivalent. This result suggests that the significant factor in the decrease in ionic conductivity is the number of end groups rather than the increase in the [Li]/[O] ratio. With the interchain interactions of the terminal LiMSSI groups, the PEG with one LiMSSI end dimerizes, and the PEG with two end groups polymerizes. These constraints are two-dimensional and slightly limit segmental motion, thus maintaining low  $T_g$ s. In contrast, a PEG with three terminal LiMSSI groups forms a three-dimensional ionic cross-linkage, which constrains the entire molecule and increases the  $T_g$ , resulting in a significant decrease in ionic conductivity.

Finally, we compared the ionic conductivity of DEG-MME-LiMSSI2 with two LiMSSI structures at one end to that of PEG200-LiMSSI2 with a similar [Li]/[O] ratio to investigate the effect of the different arrangements of the terminal LiMSSI groups on the ionic conductivity (Figure 6). The one-sided, two-terminated DEGMME-LiMSSI2 had a lower ionic

conductivity than the PEG200-LiMSSI2 with LiMSSI moieties at both ends, although the  $T_g$  was 34 K lower than that of PEG200-LiMSSI2. The low ionic conductivity of DEGMME-LiMSSI2 is probably due to the intramolecular interactions of the two terminal LiMSSI groups located within close positions. The low  $T_g$  relative to the high [Li]/[O] ratio implies a lower tendency for intermolecular interactions, which increases the freedom of chain motion. On the other hand, the intramolecular interaction between the terminal LiMSSI groups would confine the lithium ions within the molecule to suppress the intermolecular transfer of lithium ions.

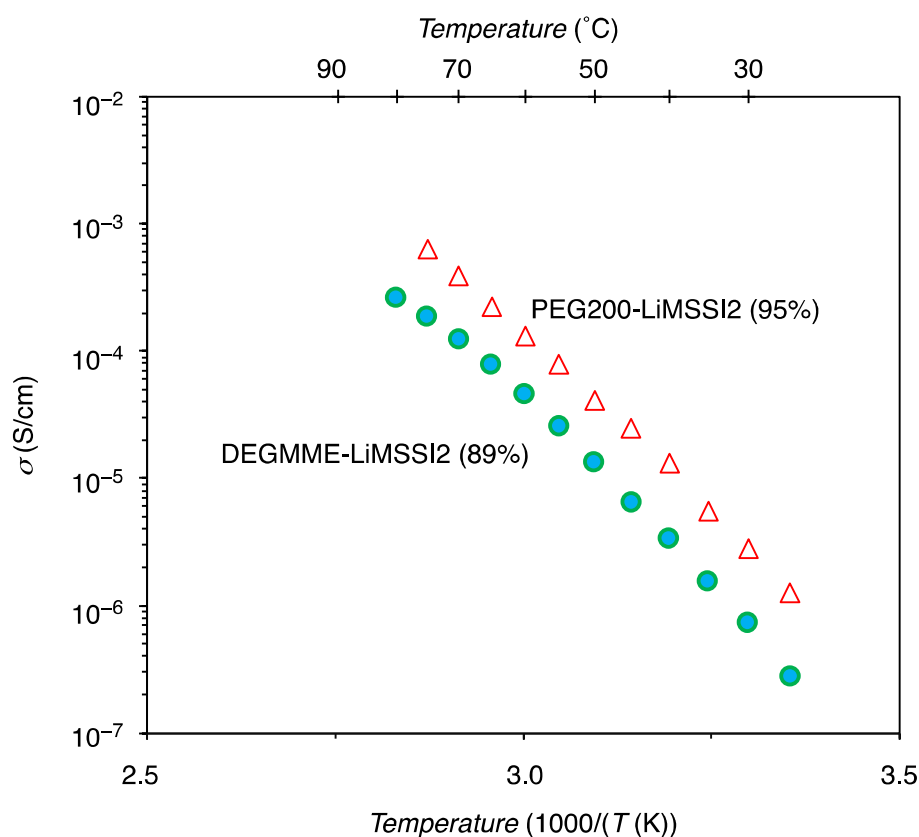


**Figure 6.** The ionic conductivities of DEG-MME-LiMSSI2 (green circle) and PEG200-LiMSSI2 (red triangle).

The ion conductivities of the examined materials are summarized in Table 2, together with those of some previously reported single-component PEG-based electrolytes. However, an exact comparison between different reports is not possible since ion conductivities are severely influenced by absorbed water [18], and measurements without appropriate drying overestimate ion conductivities (Figure S9). The ionic conductivities of fluorine-free polyelectrolytes are mostly in the range of  $10^{-6}$ – $10^{-7}$  S/cm at ambient temperature, while those of fluorine-containing polyelectrolytes are almost an order of magnitude higher. Our PEG-LiMSSI derivatives with lower  $T_g$ s are in a higher range among fluorine-free single-component polyelectrolytes. In contrast, the derivatives with higher  $T_g$ s, namely PEG-LiMSSI with multiple LiMSSI ends and a quantitative introduction efficiency, exhibited lower ionic conductivities.

**Table 2.** The ionic conductivities of the LiMSSI-terminated PEG examined in this research and the reported polymeric electrolytes bearing anionic structures.

Category	Polymer	IE (%) <sup>a</sup>	$\sigma_{total}$ (S/cm)	$T_g$ (°C)	Ref
F-free	PEG400MME-LiMSSI1	>99	$5.5 \times 10^{-6}$ @ 30 °C $1.1 \times 10^{-4}$ @ 60 °C	−48	This work
	PEG1000MME-LiMSSI1	95	$3.0 \times 10^{-5}$ @ 30 °C $2.0 \times 10^{-4}$ @ 60 °C	−56	This work
	PEG200-LiMSSI2	95	$1.3 \times 10^{-6}$ @ 30 °C $7.8 \times 10^{-5}$ @ 60 °C	−18	This work
		>99	$1.8 \times 10^{-7}$ @ 60 °C	9	This work
	PEG400-LiMSSI2	91	$2.3 \times 10^{-7}$ @ 30 °C $4.1 \times 10^{-5}$ @ 60 °C	−30	This work
		>99	$8.1 \times 10^{-8}$ @ 30 °C $1.2 \times 10^{-5}$ @ 60 °C	−11	This work
	PEG1000-LiMSSI2	>99	$2.5 \times 10^{-6}$ @ 30 °C $5.2 \times 10^{-5}$ @ 60 °C	−18	This work
	DEGMME-LiMSSI2	89	$7.3 \times 10^{-7}$ @ 30 °C $4.5 \times 10^{-5}$ @ 60 °C	−52	This work
	TMPE450-LiMSSI3	86	$2.7 \times 10^{-7}$ @ 60 °C	−18	This work
	PEG350-(SO <sub>3</sub> Li)1	N/A	$4.45 \times 10^{-6}$ @ 30 °C	−53	[7]
	PEG600-(SO <sub>3</sub> Li)2	N/A	$1.43 \times 10^{-6}$ @ 30 °C	−31	[7]
	PEG550-SO <sub>2</sub> N(Li)CH <sub>2</sub> CH <sub>2</sub> OCH <sub>3</sub>	N/A	$2.5 \times 10^{-5}$ @ 30 °C	not reported	[8]
	PEG1900-(SO <sub>2</sub> N(Li)Ph)2	N/A	$1.08 \times 10^{-6}$ @ 30 °C $3.23 \times 10^{-6}$ @ 50 °C	Semi-crystalline ( $T_m = 27$ °C)	[9]
	Networked PEG2000-SO <sub>2</sub> N(Li)Ph	N/A	$1.40 \times 10^{-6}$ @ 30 °C $4.34 \times 10^{-6}$ @ 50 °C	Rubbery ( $T_m = 34$ °C)	[9]
	MeO(CH <sub>2</sub> CH <sub>2</sub> O) <sub>3</sub> CH <sub>2</sub> -1,2,3-triazolate	N/A	$8.0 \times 10^{-7}$ @ 30 °C	−60 >	[18]
	Li{B[O(CH <sub>2</sub> CH <sub>2</sub> O) <sub>n</sub> CH <sub>3</sub> ] <sub>3</sub> C <sub>4</sub> H <sub>9</sub> }	N/A	$2 \times 10^{-5}$ @ 30 °C	−79	[13]
F-containing	Poly(LiMSVSI-co-PEGMA)	N/A	$8.4 \times 10^{-5}$ @ 25 °C $9.2 \times 10^{-4}$ @ 70 °C	−62	[31]
	Li <sup>+</sup> {Al[(OCH <sub>2</sub> CH <sub>2</sub> ) <sub>n</sub> OMe] <sub>2</sub> (SO <sub>2</sub> CF <sub>3</sub> ) <sub>2</sub> } <sup>−</sup> (n = 11.8)	N/A	$4.9 \times 10^{-5}$ @ 30 °C	−53	[10]
	Li <sup>+</sup> {B[(OCH <sub>2</sub> CH <sub>2</sub> ) <sub>4</sub> OMe] <sub>2</sub> HFIP <sub>2</sub> } <sup>−</sup>	N/A	$4.6 \times 10^{-6}$ @ 30 °C	−54	[11]
	MeOPEG550OCF <sub>2</sub> CFHOFCF <sub>2</sub> CF <sub>2</sub> SO <sub>2</sub> N(Li)SO <sub>2</sub> CF <sub>3</sub>	N/A	$5.3 \times 10^{-6}$ @ 30 °C	not reported	[16]
	MeO(CH <sub>2</sub> CH <sub>2</sub> O) <sub>12</sub> C <sub>6</sub> H <sub>4</sub> SO <sub>2</sub> N(Li)SO <sub>2</sub> CF <sub>3</sub>	N/A	$7.1 \times 10^{-6}$ @ 30 °C	−38	[17]
	Li <sup>+</sup> {B[(OCH <sub>2</sub> CH <sub>2</sub> ) <sub>3</sub> OMe] <sub>2</sub> -HFIP-Bu <sup>t</sup> } <sup>−</sup>	N/A	$1.89 \times 10^{-4}$ @ 25 °C	not reported (liquid)	[15]
	P(EOMA-co-FBSALi)	N/A	$4.0 \times 10^{-4}$ @ 30 °C	−51	[33]
	P(LiSTFSI-co-MPEGA)	N/A	$7.7 \times 10^{-6}$ @ 25 °C $1.0 \times 10^{-4}$ @ 60 °C	−47	[19]
	LiPSTFSI- <i>b</i> -PEO- <i>b</i> -LiPSTFSI	N/A	$1.3 \times 10^{-5}$ @ 60 °C	−25	[20]

<sup>a</sup> Introduction efficiency calculated using <sup>1</sup>H NMR spectroscopy. Abbreviations: HFIP, hexafluoroisopropoxy; P(EOMA-co-FBSALi), poly(ethylene oxide methoxy acrylate-co-lithium 1,1,2-trifluorobutanesulfonate acrylate); LiSTFSI, lithium (4-styrenesulfonyl)(trifluoromethanesulfonyl imide); MPEGA, methoxy polyethylene glycol acrylate; LiPSTFSI, lithium(4-styrenesulfonyl)(trifluoromethyl(S-trifluoromethylsulfonylimino) sulfonyl)imide; N/A, not available.

The logarithms of the ionic conductivities of our materials at 60 °C correlate well with the  $T_g$ s, except for DEGMME-LiMSSI2 and TPME450-LiMSSI3, which have low ionic conductivities relative to their  $T_g$ s (Figure 7). The  $R^2$  values for the linear correlations are 0.42 and 0.80 for all the examined derivatives and the derivatives except DEGMME-LiMSSI2 and TPME450-LiMSSI3, respectively. This correlation implies that the ionic conduction in PEGxMME-LiMSSI1 and PEGx-LiMSSI2 proceeds in an identical mechanism. Intramolecular and three-dimensional ionic interactions negatively affected the ionic conduction behaviors.

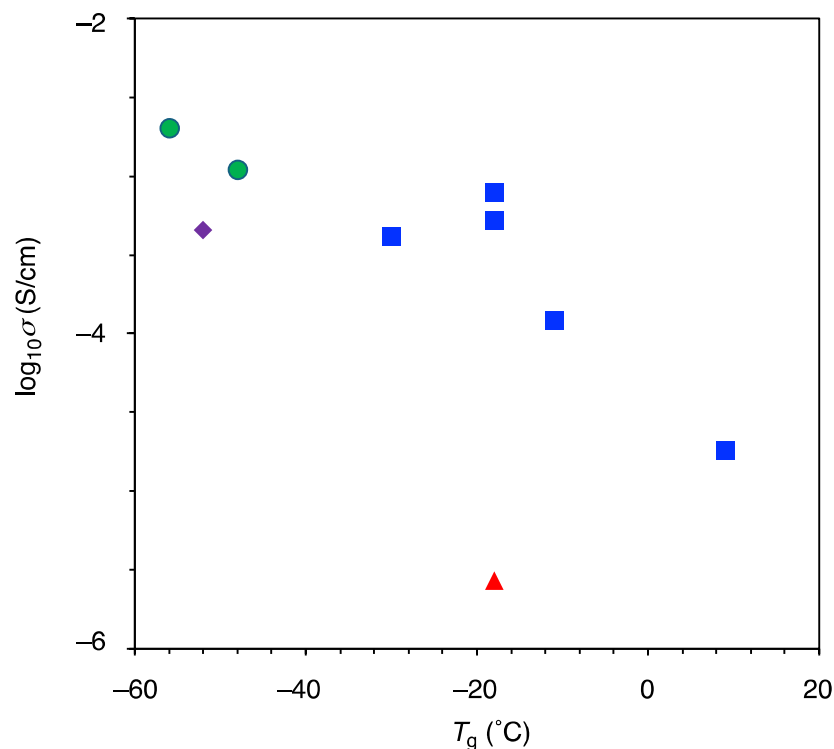


**Figure 7.** The ionic conductivities of the PEG-LiMSSI derivatives in this study. Mono-LiMSSI terminal (green circle), both-end type two LiMSSI termini (blue square), single-end type two LiMSSI termini (purple rhombus), and three LiMSSI termini (red triangle) PEG derivatives.

Based on these results, we suggest PEG<sub>x</sub>MME-LiMSSI1 and PEG<sub>x</sub>-LiMSSI2 containing a trace amount of an unreacted end to improve the mobility of the chains as suitable single-component polyelectrolytes.

#### 4. Conclusions

Fluorine-free single-component polyelectrolytes were developed by introducing LiMSSI moieties to PEG derivatives with one, two, and three LiMSSI termini via the simultaneous Michael-type addition and lithiation of PEGs and MSVSI. The ionic conductivities at 60  $^{\circ}\text{C}$  ranged from  $1.8 \times 10^{-7}$  to  $2.0 \times 10^{-4}$  S/cm. PEG-LiMSSI derivatives with one LiMSSI terminus (PEG<sub>x</sub>MME-LiMSSI1) and two LiMSSI termini at both ends (PEG<sub>x</sub>-LiMSSI2) exhibited higher ionic conductivity than those with two LiMSSI termini at one end (DEGMME-LiMSSI2) and with three LiMSSI termini (TPME450-LiMSSI3), and their ionic conductivities correlated well with their  $T_g$ s. The low ionic conductivities of DEGMME-LiMSSI2 and TPME450-LiMSSI3 probably result from the restriction of the mobility of lithium cation via intermolecular and networked ionic interactions, respectively. PEG<sub>x</sub>MME-LiMSSI1 and PEG<sub>x</sub>-LiMSSI show good ionic conductivity as fluorine-free single-component polyelectrolytes without additional salts and solvents.

This work revealed the effect of the structural variance of a series of PEG derivatives with anionic end moieties on ionic conductivities, which is informative for the design of single-component polyelectrolytes. The remaining task for the further optimization of our materials is the evaluation of the transference numbers of  $\text{Li}^+$ , which are expected to be higher than 0.4, similar to that reported in polyelectrolytes due to the suppressed transport of anions. In addition, the suppression of intermolecular ionic interactions without intramolecular interactions will also lower the  $T_g$  and, thus, improve ionic conductivities. These investigations will contribute to the development of fluorine-free polyelectrolytes for sustainable electronics.

**Supplementary Materials:** The following supporting information can be downloaded at: <https://www.mdpi.com/article/10.3390/technologies12050065/s1>, Figures S1–S6: <sup>1</sup>H NMR spectra of PEG-LiMSSI derivatives; Figure S7. Cyclic voltammograms of DEGMME-LiMSSI2 and TPME450-LiMSSI3; Figure S8: DSC curves of polyelectrolytes; Figure S9: ionic conductivity of PEG-LiMSSI with insufficient drying.

**Author Contributions:** Conceptualization, B.O.; methodology, B.O., K.H., Y.F. and Y.M.; software, B.O., K.H. and Y.F.; validation, B.O., K.H., Y.F. and Y.M.; formal analysis, K.H. and Y.F.; investigation, K.H. and Y.F.; resources, B.O. and Y.M.; data curation, B.O., K.H. and Y.F.; writing—original draft preparation, B.O., K.H. and Y.F.; writing—review and editing, B.O. and Y.M.; visualization, B.O., K.H. and Y.F.; supervision, B.O.; project administration, B.O.; funding acquisition, B.O. and Y.M. All authors have read and agreed to the published version of the manuscript.

**Funding:** This research received no external funding.

**Institutional Review Board Statement:** Not applicable.

**Informed Consent Statement:** Not applicable.

**Data Availability Statement:** All the data substantiating the conclusion of this study are included. Other primary data are available upon reasonable request from the corresponding author.

**Acknowledgments:** The authors are grateful to Hideharu Mori of Yamagata University for his kind assistance in ionic conductivity measurements.

**Conflicts of Interest:** The authors declare no conflicts of interest.

## References

1. Murata, K.; Izuchi, S.; Yoshihisa, Y. An overview of the research and development of solid polymer electrolyte batteries. *Electrochim. Acta* **2000**, *45*, 1501. [[CrossRef](#)]
2. Xu, K. Electrolytes and interphases in Li-ion batteries and beyond. *Chem. Rev.* **2014**, *114*, 11503–11618. [[CrossRef](#)] [[PubMed](#)]
3. Zhang, H.; Li, C.; Piszcz, M.; Coysa, E.; Rojo, T.; Rodriguez-Martinez, L.M.; Armand, M.; Zhou, Z. Single lithium-ion conducting solid polymer electrolytes: Advances and perspectives. *Chem. Soc. Rev.* **2017**, *46*, 797–815. [[CrossRef](#)]
4. Tong, B.; Song, Z.; Wu, H.; Wang, X.; Feng, W.; Zhou, Z.; Zhang, H. Ion transport and structural design of lithium-ion conductive solid polymer electrolytes: A perspective. *Mater. Futures* **2022**, *1*, 042103. [[CrossRef](#)]
5. Ohno, H.; Ito, K. Poly(ethylene oxide)s having carboxylate groups on the chain end. *Polymer* **1995**, *36*, 891–893. [[CrossRef](#)]
6. Ito, K.; Tominaga, Y.; Ohno, H. Polyether/salt hybrid (IV). Effect of benzenesulfonate group(s) and PEO molecular weight on the bulk ionic conductivity. *Electrochim. Acta* **1997**, *42*, 1561–1570. [[CrossRef](#)]
7. Ito, K.; Nishina, N.; Ohno, H. High lithium ionic conductivity of poly(ethylene oxide)s having sulfonate groups on their chain ends. *J. Mater. Chem.* **1997**, *7*, 1357–1362. [[CrossRef](#)]
8. Tominaga, Y.; Ohno, H. High ionic conductivity of PEO/sulfonamide salt hybrids. *Solid State Ion.* **1999**, *124*, 323–329. [[CrossRef](#)]
9. Tominaga, Y.; Ohno, H. Lithium ion conduction in linear- and network-type polymers of PEO/sulfonamide salt hybrids. *Electrochim. Acta* **2000**, *45*, 3081–3086. [[CrossRef](#)]
10. Fujinami, T.; Buzoujima, Y. Novel lithium salts exhibiting high lithium ion transference numbers in polymer electrolytes. *J. Power Sources* **2003**, *119–121*, 438–441. [[CrossRef](#)]
11. Shobukawa, H.; Tokuda, H.; Tabata, S.; Watanabe, M. Preparation and transport properties of novel lithium ionic liquids. *Electrochim. Acta* **2004**, *50*, 305–309. [[CrossRef](#)]
12. Zygadło-Monikowska, E.; Florjańczyk, Z.; Ostrowska, J.; Bołtomiuk, P.; Frydrych, J.; Sadurski, W.; Langwald, N. Synthesis and characterization of new trifluoroalkoxyborates lithium salts of ionic liquid properties. *Electrochim. Acta* **2011**, *57*, 66–73. [[CrossRef](#)]
13. Zygadło-Monikowska, E.; Florjańczyk, Z.; Służewska, K.; Ostrowska, J.; Langwald, N.; Tomaszewska, A. Lithium conducting ionic liquids based on lithium borate salts. *J. Power Sources* **2010**, *195*, 6055–6061. [[CrossRef](#)]
14. Zygadło-Monikowska, E.; Florjańczyk, Z.; Tomaszewska, A.; Pawlicka, M.; Langwald, N.; Kovarsky, R.; Mazor, H.; Golodnitsky, D.; Peled, E. New boron compounds as additives for lithium polymer electrolytes. *Electrochim. Acta* **2007**, *53*, 1481–1489. [[CrossRef](#)]
15. Guzmán-González, G.; Alvarez-Tirado, M.; Olmedo-Martínez, J.L.; Picchio, M.L.; Casado, N.; Forsyth, M.; Mecerreyes, D. Lithium borate ionic liquids as single-component electrolytes for batteries. *Adv. Energy Mater.* **2023**, *13*, 2202974. [[CrossRef](#)]
16. Hallac, B.B.; Geiculescu, O.E.; Rajagopal, R.V.; Creager, S.E.; DesMarteau, D.D. Lithium-conducting ionic melt electrolytes from polyether-functionalized fluorosulfonamide anions. *Electrochim. Acta* **2008**, *53*, 5985–5991. [[CrossRef](#)]
17. Herath, M.B.; Creager, S.E.; Rajagopal, R.V.; Geiculescu, O.E.; DesMarteau, D.D. Ionic conduction in polyether-based lithium arylfluorosulfonimide ionic melt electrolytes. *Electrochim. Acta* **2009**, *54*, 5877–5883. [[CrossRef](#)]
18. Flachard, D.; Rolland, J.; Obadia, M.M.; Serghei, A.; Bouchet, R.; Drockenmuller, E. A 1,2,3-triazolate lithium salt with ionic liquid properties at room temperature. *Chem. Commun.* **2018**, *54*, 9035–9038. [[CrossRef](#)] [[PubMed](#)]

19. Feng, S.W.; Shi, D.Y.; Liu, F.; Zheng, L.P.; Nie, J.; Feng, W.F.; Huang, X.J.; Armand, M.; Zhou, Z.B. Single lithium-ion conducting polymer electrolytes based on poly[(4-styrenesulfonyl)(trifluoromethanesulfonyl)imide] anions *Electrochim. Acta* **2013**, *93*, 254–263.
20. Bouchet, R.; Maria, S.; Meziane, R.; Aboulaich, A.; Lienafa, L.; Bonnet, J.-P.; Phan, T.N.T.; Bertin, D.; Gignes, D.; Devaux, D.; et al. Single-ion BAB triblock copolymers as highly efficient electrolytes for lithium-metal batteries. *Nat. Mater.* **2013**, *12*, 452–457. [[CrossRef](#)]
21. Ma, Q.; Zhang, H.; Zhou, C.; Zheng, L.; Cheng, P.; Nie, J.; Feng, W.; Hu, Y.-S.; Li, H.; Huang, X.; et al. Single lithium-ion conducting polymer electrolytes based on a super-delocalized polyanion. *Angew. Chem. Int. Ed.* **2016**, *55*, 2521–2525. [[CrossRef](#)]
22. Matsumoto, K.; Endo, T. Design and synthesis of ionic-conductive epoxy-based networked polymers. *React. Funct. Polym.* **2013**, *73*, 278–282. [[CrossRef](#)]
23. Ankley, G.T.; Cureton, P.; Hoke, R.A.; Houde, M.; Kumar, A.; Kurias, J.; Lanno, R.; McCarthy, C.; Newsted, J.; Salice, C.J.; et al. Assessing the Ecological risks of per- and polyfluoroalkyl substances: Current state-of-the science and a proposed path forward. *Environ. Toxicol. Chem.* **2021**, *40*, 564–605. [[CrossRef](#)] [[PubMed](#)]
24. Brunn, H.; Arnold, G.; Körner, W.; Rippen, G.; Steinhäuser, K.G.; Valentin, I. PFAS: Forever chemicals—Persistent, bioaccumulative and mobile. Reviewing the status and the need for their phase out and remediation of contaminated sites. *Environ. Sci. Eur.* **2023**, *35*, 20. [[CrossRef](#)]
25. Mandal, B.; Sooksimuang, T.; Griffin, B.; Padhi, A.; Filler, R. New lithium salts for rechargeable battery electrolytes. *Solid State Ion.* **2004**, *175*, 267–272. [[CrossRef](#)]
26. Scheers, J.; Lim, D.-H.; Kim, J.-K.; Paillard, E.; Henderson, W.A.; Johansson, P.; Ahn, J.-H.; Jacobsson, P. All fluorine-free lithium battery electrolytes. *J. Power Sources* **2014**, *251*, 451–458. [[CrossRef](#)]
27. Hosseini-Bab-Anari, E.; Boschin, A.; Mandai, T.; Masu, H.; Moth-Poulsen, K.; Johansson, P. Fluorine-free salts for aqueous lithium-ion and sodium-ion battery electrolytes. *RSC Adv.* **2016**, *6*, 85194–85201. [[CrossRef](#)]
28. He, X.; Yan, B.; Zhang, X.; Liu, Z.; Bresser, D.; Wang, J.; Wang, R.; Cao, X.; Su, Y.; Jia, H.; et al. Fluorine-free water-in-ionomer electrolytes for sustainable lithium-ion batteries. *Nat. Commun.* **2018**, *9*, 5320. [[CrossRef](#)]
29. Martinez-Ibañez, M.; Sanchez-Diez, E.; Qiao, L.; Meabe, L.; Santiago, A.; Zhu, H.; O'Dell, L.A.; Carrasco, J.; Forsyth, M.; Armand, M.; et al. Weakly coordinating fluorine-free polysalt for single lithium-ion conductive solid polymer electrolytes. *Batter. Supercaps* **2020**, *3*, 738–746. [[CrossRef](#)]
30. Hernández, G.; Mogensen, R.; Younesi, R.; Mindemark, J. Fluorine-free electrolytes for lithium and sodium batteries. *Batter. Supercaps* **2022**, *5*, e202100373. [[CrossRef](#)]
31. Matsumura, Y.; Shiraiwa, T.; Hayasaka, T.; Yoshida, S.; Ochiai, B. Synthesis of fluorine-free highly ion conductive polymer electrolyte having lithium bisulfonimide unit. *J. Electrochem. Soc.* **2018**, *165*, B3119–B3121. [[CrossRef](#)]
32. Nakatsuji, Y.; Nakamura, T.; Okahara, M.; Dishong, D.M.; Gokel, G.W. Crown cation complex effects. 22. Enhancement of cation binding in lariat ethers bearing a methyl group at the quaternary, pivot carbon atom. *J. Org. Chem.* **1983**, *48*, 1237–1242. [[CrossRef](#)]
33. Cowie, J.; Spence, G. Novel single ion, comb-branched polymer electrolytes. *Solid State Ion.* **1999**, *123*, 233–242. [[CrossRef](#)]

**Disclaimer/Publisher's Note:** The statements, opinions and data contained in all publications are solely those of the individual author(s) and contributor(s) and not of MDPI and/or the editor(s). MDPI and/or the editor(s) disclaim responsibility for any injury to people or property resulting from any ideas, methods, instructions or products referred to in the content.